

4-2006

# Thermometric Measurements of the Molecular Sublayer at the Air-Water Interface

B. Ward

*Old Dominion University*

Follow this and additional works at: [https://digitalcommons.odu.edu/oeas\\_fac\\_pubs](https://digitalcommons.odu.edu/oeas_fac_pubs)

 Part of the [Geology Commons](#), [Geophysics and Seismology Commons](#), and the [Oceanography Commons](#)

---

## Repository Citation

Ward, B., "Thermometric Measurements of the Molecular Sublayer at the Air-Water Interface" (2006). *OEAS Faculty Publications*. 271. [https://digitalcommons.odu.edu/oeas\\_fac\\_pubs/271](https://digitalcommons.odu.edu/oeas_fac_pubs/271)

## Original Publication Citation

Ward, B., & Donelan, M. A. (2006). Thermometric measurements of the molecular sublayer at the air-water interface. *Geophysical Research Letters*, 33(7), L07605. doi:10.1029/2005gl024769

This Article is brought to you for free and open access by the Ocean, Earth & Atmospheric Sciences at ODU Digital Commons. It has been accepted for inclusion in OEAS Faculty Publications by an authorized administrator of ODU Digital Commons. For more information, please contact [digitalcommons@odu.edu](mailto:digitalcommons@odu.edu).

## Thermometric measurements of the molecular sublayer at the air-water interface

B. Ward<sup>1</sup> and M. A. Donelan<sup>2</sup>

Received 26 September 2005; revised 24 February 2006; accepted 6 March 2006; published 11 April 2006.

[1] A series of measurements was conducted in the Air-Sea Interaction Saltwater Tank (ASIST) to study the response of the air-water interfacial molecular sublayer under various heat flux and wind speed conditions. In-situ gradients were measured with a platinum-plated tungsten wire microthermometer, which resolved the temperature of the thermally conductive sublayer. Air-sea heat flux was controlled by changing the air-water temperature difference ( $\Delta T^{AW}$ ) and the wind speed, and measurements were made for three  $\Delta T^{AW}$  regimes over a range of wind speeds. A function was fitted to the measured temperature profiles as a way of extracting the boundary layer thickness in a consistent fashion, from which the  $\lambda$  coefficient after Saunders (1967) was computed. This dataset returned a mean  $\lambda$  coefficient of  $2.4 \pm 0.5$ , which was generally lower than previous studies, and was found to be independent of wind speed in the range of 1 to 9  $\text{ms}^{-1}$ . **Citation:** Ward, B., and M. A. Donelan (2006), Thermometric measurements of the molecular sublayer at the air-water interface, *Geophys. Res. Lett.*, 33, L07605, doi:10.1029/2005GL024769.

### 1. Introduction

[2] As the air-water interface is approached from the water side, turbulent motion is suppressed [Donelan and Wanninkhof, 2002]. Heat flow from the ocean to the atmosphere results in a thin conductive layer where the temperature profile is linear with depth [McLeish and Putland, 1975]. The upper bound of this layer is known as the skin temperature, most commonly measured by infrared devices, which, due to the absorption properties of water in that part of the electromagnetic spectrum, measure temperature in only the top few micrometers of water. The difference between the skin temperature  $T_{skin}$  and the temperature at depth  $T_{depth}$  is  $\Delta T^{SD}$ , and is defined here as  $\Delta T^{SD} = T_{skin} - T_{depth}$ .

[3] Saunders [1967] was the first to present a theory to account for  $\Delta T^{SD}$ . With the underlying assumption that the heat transfer across the thermal sublayer occurs by molecular conduction, the temperature gradient is given by:

$$\Delta T^{SD} = \frac{Q_n \delta_c}{k} \quad (1)$$

where  $Q_n$  is the net air-sea heat flux in the absence of insolation,  $\delta_c$  is the thickness of the (thermally) conductive

sublayer, and  $k$  the thermal conductivity of water. Since turbulence is responsible for the transport of momentum as well as heat, the implication is that a viscous sublayer must also exist at the surface. Grassl [1976] schematically described these different sublayers. Embedded within the viscous sublayer  $\delta_v$  is the thermal sublayer  $\delta_c$ . Using dimensional analysis, Saunders [1967] derived an expression for the thickness of the viscous sublayer:

$$\delta_v \sim \nu \left( \frac{\tau}{\rho_w} \right)^{-1/2} \sim \frac{\nu}{u_*} \quad (2)$$

where  $\nu$  is the kinematic viscosity of seawater,  $\tau$  is the wind stress, and  $u_*$  is the sea surface friction velocity. The combination of equations (1) and (2) gives:

$$\Delta T^{SD} = \frac{Q_n}{k} \lambda \frac{\nu}{(\rho_a/\rho_w)^{1/2} u_{*a}}$$

and

$$\lambda = \frac{\delta_c (\rho_a/\rho_w)^{1/2} u_{*a}}{\nu} \quad (3)$$

where  $\rho_a$  is the density of air,  $\rho_w$  is seawater density, and  $u_{*a}$  is the atmospheric friction velocity. The  $\lambda$  coefficient was introduced by Saunders [1967] to account for the difference in stress on both sides of the interface. Several studies have suggested that  $\lambda$  depends on conditions [Fairall et al., 1996]. Grassl [1976] suggested that  $\lambda$  accounts for the difference in the thicknesses of  $\delta_c$  and  $\delta_v$ .

[4] The  $\lambda$  coefficient has received the attention of a number of researchers [see Federov and Ginsburg, 1992, Table 3.3; Robinson et al., 1984, Table 4]. In this study, we present estimates of  $\lambda$  using data from a microthermometer during the Skin Layer Experiment in the Air-Sea Interaction Saltwater Tank (ASIST). These in-situ, thermometric observations provided direct measurements of the thickness of the conductive layer ( $\delta_c$ ), thus allowing a unique method of estimating  $\lambda$  according to equation (3). The objectives of the experiment were to investigate the behavior of the molecular sublayer under varying heat flux and wind speed regimes. Since molecular conduction is the dominant process, it can be argued that equations (1) and (3) are equally applicable in both the laboratory and the ocean [Paulson and Parker, 1972]. In section 2, we describe the experiment and the measurements of the sublayer. In section 3 we discuss the results in relation to other studies, and in section 4 we present our conclusions.

### 2. Profiles of Molecular Sublayer

[5] The ASIST wind-wave tank has a working section of 15 m and cross section of  $1 \times 1$  m. It is constructed with

<sup>1</sup>Department of Ocean, Earth and Atmospheric Sciences, Old Dominion University, Norfolk, Virginia, USA.

<sup>2</sup>Division of Applied Marine Physics, Rosenstiel School of Marine and Atmospheric Science, University of Miami, Miami, Florida, USA.

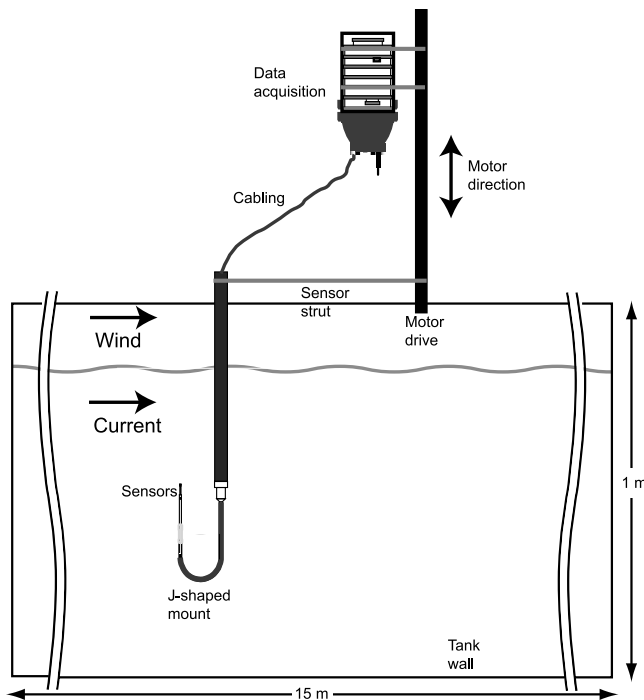


**Figure 1.** Schematic of the profiling setup during the Skin Layer Experiment in the Air-Sea Interaction Saltwater Tank.

transparent acrylic panels to allow visualization of installed instrumentation and flow. The water depth in ASIST may be varied from 25 cm to 50 cm, and either fresh or salt water may be used. The re-circulating water tunnel is driven by a pump and currents of up to  $40 \text{ cm s}^{-1}$  may be generated. A computer-controlled hydraulic wave-maker for wave-field generation is available. The water temperature is controlled by a heat exchanger in the range of  $2^\circ\text{C}$  to  $40^\circ\text{C}$ . The wind tunnel of ASIST may be operated in either closed (re-circulating) or open (once through) modes and the maximum center-line wind speeds are, respectively,  $30$  and  $22 \text{ ms}^{-1}$ .

[6] During the Skin Layer Experiment, fresh water was used as there was no compelling scientific advantage to using saltwater. The wind tunnel was in the open mode to allow steady state fluxes to be obtained. This pumped air at the ambient external temperature into the tank, which remained fairly constant for the two week experiment. The  $\Delta T^{AW}$  was controlled by changing the water temperature, and for each regime, the wind speed was varied over a range of  $1$  to  $10 \text{ ms}^{-1}$ .

[7] Thermometric measurements of the molecular sublayer were conducted with a fine wire microthermometer, whose sensing element was platinum-plated tungsten of diameter  $5 \mu\text{m}$ , and length  $1.2 \text{ mm}$ . The microthermometer was found to be delicate, and corroded over time. This required frequent sensor replacement making participation during all the experimental runs impractical.

[8] There was significant variability in the microthermometer temperature data. This is attributed to surface renewal events continuously occurring within the molecular boundary layer, replacing water at the interface with a parcel of bulk water. It is therefore necessary in this type of

measurement to average the profiles so as to reduce the randomness from the surface renewal process.

[9] Absolute temperature was provided by a FP07 thermistor, and the surface was detected with a microconductivity sensor (see *Ward et al.* [2004] for a full description of the sensors). The sensors were mounted into J-shaped supports, which were attached to a vertical mast coupled to a linear servo motor (Figure 1). Measurements were made from a depth of about  $10 \text{ cm}$  through the surface, at an ascent velocity of  $0.5 \text{ ms}^{-1}$  and at a repetition period of  $5$  seconds. For each run, profiles were acquired for  $4$  minutes. Drifts in absolute temperature for the microthermometer were corrected through the application of an offset derived from a calibrated FP07 thermistor.

[10] In order to extract the relevant parameters from each profile (i.e. the conductive sublayer thickness  $\delta_c$ ), each of the individual profiles were fitted to the function provided by *Howard* [1966]. This theoretical profile is an error function solution to the diffusion equation, given by:

$$\frac{T(z/\delta_c) - T_{depth}}{\Delta T^{SD}} = (1 + 2\zeta^2)\text{erfc}\zeta - 2\pi^{-1/2}\zeta e^{-\zeta^2} \quad (4)$$

where  $\zeta = (\sqrt{\pi}/4)(z/\delta_c)$ , and  $z$  is depth. The model can reproduce the averaged profile when the correct choice of  $\delta_c$  and  $\Delta T^{SD}$  values are used.

[11] There were a total of ten successful runs and these are graphed in Figure 2 showing average temperature profiles and standard deviations from the mean. The modelled profiles from equation (4) are also included in Figure 2. Table 1 shows the nominal conditions during each run (wind speed and  $\Delta T^{AW}$ ), as well as the derived mean sublayer thickness  $\delta_c$ . Calculation of  $\lambda$  in equation (3) also required determination of the friction velocity, which was derived by *Ocampo-Torres et al.* [1994], who studied exchange coefficients in a wind-wave tank similar to ASIST. Both  $u_*$  and  $\lambda$  values for each run are also shown in Table 1. Both the  $\delta_c$  and  $\lambda$  are shown with their standard deviations deduced from the individual profiles in each run.

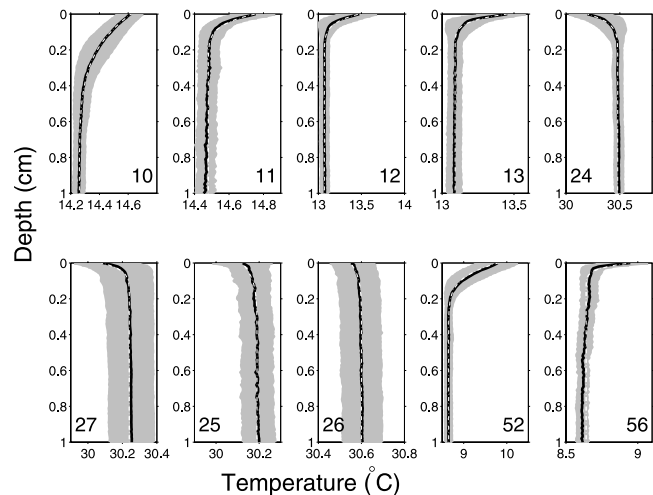


**Figure 2.** Average temperature profiles for each run (run numbers indicated). The shaded areas represent one standard deviation from the mean profile (solid line). The white dashed line is the modelled profile from equation (4).

**Table 1.** Nominal Conditions During the Runs and the Derived Profile Parameters<sup>a</sup>

Regime	Run No.	$T_a - T_w$ , °C	$u$ ms <sup>-1</sup>	$u_*$ , ms <sup>-1</sup>	$\bar{\delta}_c$	$\bar{\lambda}$	$\bar{r}$
1	10	+10	1	0.0016	2.16 ± 1.09	2.93 ± 1.48	0.98
1	11	+10	3	0.0032	0.55 ± 0.25	1.52 ± 0.68	0.90
1	12	+10	5	0.0058	0.39 ± 0.19	1.93 ± 0.96	0.95
1	13	+10	7	0.0093	0.36 ± 0.25	2.85 ± 1.95	0.92
2	24	-5	4	0.0044	0.44 ± 0.27	2.45 ± 1.50	0.87
2	27	-5	5	0.0058	0.40 ± 0.33	2.94 ± 2.44	0.79
2	25	-5	7	0.0093	0.83 ± 0.50	9.72 ± 5.82	0.47
2	26	-5	10	0.0161	0.41 ± 0.22	8.35 ± 4.52	0.43
3	52	+15	3	0.0033	0.85 ± 0.36	2.04 ± 0.86	0.97
3	56	+15	9	0.0137	0.26 ± 0.14	2.64 ± 1.38	0.80

<sup>a</sup>Here  $\Delta T^{AW}$  is the air-water temperature difference,  $T_a$  and  $T_w$  the air and water temperatures,  $u$  is the wind speed,  $u_*$  the friction velocity after *Ocampo-Torres et al.* [1994],  $\bar{\delta}_c$  is the mean sublayer thickness from the data presented in Figure 2, the mean values of the  $\bar{\lambda}$  coefficient, and  $\bar{r}$  the mean correlation coefficient between the measured temperature profiles and the model from equation (4).

Runs 25 and 26 show much larger standard deviations than the eight other runs, as well as lower mean correlation coefficients, and therefore provide relatively unreliable estimates of the means. These two runs are not included in the subsequent analysis.

### 3. Results and Discussion

[12] The results of this study are presented in Figure 3, where mean values of the thermal sublayer thickness  $\delta_c$  and the  $\lambda$  coefficient are plotted against wind speed. The  $\delta_c$  values are measured directly with the microthermometer and exhibit an exponential relationship with wind speed. The  $\lambda$  values were calculated according to (3). The  $\lambda$  coefficient appears to be essentially independent of wind speed in the range of 1 to 9 ms<sup>-1</sup> with a mean value of  $2.4 \pm 0.5$ .

[13] Also shown in Figure 3 are the estimates of  $\lambda$  from previous studies: *Saunders* [1967] (S67), *Hasse* [1971] (H71), *Paulson and Parker* [1972] (PP72), *Grassl* [1976] (G76), *Paulson and Simpson* [1981] (PS81), *Wu* [1985] (W85), *Schlüssel et al.* [1990] (S90), *Soloviev and Schlüssel* [1994] (SS94), and *Kent et al.* [1996] (K96). All of these studies used equation (1) to estimate  $\lambda$ . Three of the authors (H71, PP72, PS81) found  $\lambda$  to be constant over the range of conditions encountered. The results given by G76 and W85 both presented two regimes for  $\lambda$ , with slopes differing above the critical wind speeds of 4 and 7 ms<sup>-1</sup>, respectively. The remaining studies (S90, SS94, K96) presented  $\lambda$  values from measurements in the field.

[14] H71 independently derived a model, but the main difference to *Saunders* [1967, equation (1)] was the temperature dependency of  $\nu$ . The model and observations presented by H71 were in excellent agreement to, and the  $\lambda$  coefficient was found to have a constant value of  $\lambda = 8$  over the wind speed range of 1.5–11 ms<sup>-1</sup>. The only other laboratory study was given by PP72, who made radiometric measurements of a water bath over which air was blown at a constant velocity. The average value of  $\lambda$  given by PP72 was found to be  $15 \pm 1$  for a 1.3 to 3.6 ms<sup>-1</sup> wind speed range. PS81 found a value for  $\lambda = 6.5 \pm 0.6$  over a wind speed range of 3–11 ms<sup>-1</sup> from measurements on R/P FLIP. These constant  $\lambda$  values (8, 15, and 6.5) are considerably larger than the  $\lambda = 2.4$  value from this study.

[15] G76 used field data from a Barnes PRT-5 radiometer during the GATE experiment. G76 used a total of 452 hours of measurements and found that there were two regimes for  $\lambda$ , where the slope was greater for the lower wind speeds. The critical wind speed was 4 ms<sup>-1</sup>. W85 reanalyzed data given by G76, *Simpson and Clayton* [1980], and PS81 and fitted a function, where he found that  $\lambda$  increased linearly from 2–7 over a 0–7 ms<sup>-1</sup> wind speed range, and then assumed a constant value of 7 above. Both of these studies had  $\lambda$  values larger than this study.

[16] S90 determined  $\lambda$  from field measurements, and found that for a constant  $\lambda = 4.5$ , the correlation coefficient between expression (1) and the data was 0.26, but when  $\lambda$  was allowed to vary, a correlation of 0.75 was achieved. SS94 used surface renewal to develop a model for  $\Delta T$  for three wind speed regimes. Using the same data given by

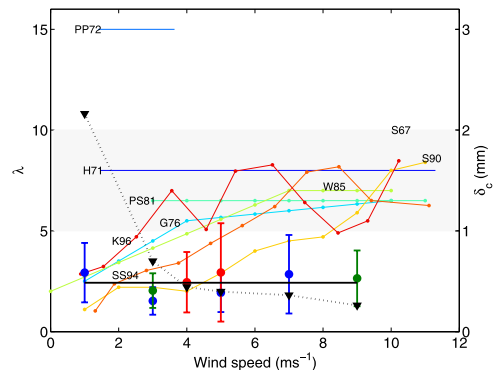


**Figure 3.** Mean values of the  $\lambda$  coefficient as a function of wind speed for each of the runs (error bars represent 1 standard deviation from the mean). Data points from the Skin Layer Experiment are represented by blue (regime 1), red (regime 2), and green (regime 3), according to Table 1. Also shown are estimates of  $\lambda$  from *Saunders* [1967] (S67), *Hasse* [1971] (H71), *Paulson and Parker* [1972] (PP72), *Grassl* [1976] (G76), *Paulson and Simpson* [1981] (PS81), *Wu* [1985] (W85), *Schlüssel et al.* [1990] (S90), *Soloviev and Schlüssel* [1994] (SS94), and *Kent et al.* [1996] (K96). The solid black line represents a mean  $\lambda$  value of 2.4. The black dashed line is the mean value of  $\delta_c$  (right-hand axis) for each wind speed available (see Table 1 for  $\delta_c$  values).

S90,  $\lambda$  was found to increase up to about  $8.5 \text{ ms}^{-1}$ . The values of  $\lambda$  given by K96 were also allowed to vary to provide a better fit to  $\Delta T^{SD}$  in equation (1), but there was much more variability than S90. Above  $4 \text{ ms}^{-1}$ , K96 suggested a value of 7 as a reasonable value.

[17] The values of  $\lambda$  from this study are generally lower than those from the previous estimates described above. However, our estimates are derived from direct measurements of the thickness of the molecular sublayer according to (3), whereas the previous estimates are derived from (1). It can be argued that the direct method for determining  $\lambda$  is more accurate as it does not include errors introduced from the heat flux calculations.

#### 4. Conclusions

[18] This study presents estimates of the  $\lambda$  coefficient, originally introduced by Saunders [1967] in a parameterization for determining the skin-bulk temperature difference at the ocean surface. There have been several estimates of  $\lambda$  from previous studies, which were all estimated using equation (1). Here, we present measurements at the air-water interface in the ASIST wind-wave tank using a microthermometer which possessed the resolution to provide the thickness of the conductive sublayer  $\delta_c$ . This was the first time that direct measurements of the temperature profile in the molecular boundary layer were performed to test the related theoretical framework and to give insight into the variability of  $\lambda$  coefficient. From equation (3) we estimate  $\lambda$ , and the mean value is generally found to have a much lower value compared to other studies.

[19] Fairall et al. [1996] provides a cool-skin correction for the TOGA-COARE algorithm, which is widely used for determining air-sea heat fluxes from standard meteorological measurements. The  $\lambda$  coefficient increases with wind speed until shear-driven conditions occur (at about  $6 \text{ ms}^{-1}$ ), whereupon it reaches a constant value of 6; for wind speeds of about  $2.5 \text{ ms}^{-1}$ ,  $\lambda = 4.8$  [Fairall et al., 1996]. The constant  $\lambda$  from this study will reduce the cool-skin correction thereby providing a higher flux estimate. For example, for a wind speed of about  $8 \text{ ms}^{-1}$  and a SST of  $29^\circ\text{C}$ , the increase in the nighttime cooling at the ocean surface is about  $10 \text{ Wm}^{-2}$ . Ward [2006] has shown that errors in  $T_{skin}$  can introduce errors in the resulting air-sea heat fluxes. Thus, increased accuracy in heat flux bulk formulae provides motivation for knowledge of the behavior of the  $\lambda$  coefficient.

[20] The results from this experiment are preliminary, but provide an indication as to the behavior of  $\lambda$ , as well as motivation for further studies. With improved sensor technology, a field or laboratory campaign to make estimates of  $\lambda$  from equations (1) and (3) could be carried out. This would require high accuracy radiometric measurements with on-line calibration, eddy correlation heat flux measurements to reduce the uncertainty in (1), and profiles from within the

bulk to the air-water interface with sub-millimeter, sub-millisecond, and centi-degree resolution.

[21] **Acknowledgments.** Tony Williams and Jonathan Bromley provided top level support for the development of the analog conditioning electronics for the microthermometer. Cyril McCormick, Kevin Maillet, and Mike Rebozo provided the technical support during the Skin Layer Experiment at ASIST. This work was funded by the Office of Naval Research (ONR Award N00014-03-1-0384).

#### References

- Donelan, M. A., and R. Wanninkhof (2002), Gas transfer at water surfaces: Concepts and issues, in *Gas Transfer at Water Surfaces*, *Geophys. Monogr. Ser.*, vol. 127, edited by M. A. Donelan et al., pp. 1–10, AGU, Washington, D. C.
- Fairall, C. W., E. F. Bradley, J. S. Godfrey, G. A. Wick, J. B. Edson, and G. S. Young (1996), Cool-skin and warm-layer effects on sea surface temperature, *J. Geophys. Res.*, *101*, 1295–1308.
- Federov, K. N., and A. I. Ginsburg (1992), *The Near-Surface Layer of the Ocean*, 256 pp., E. J. Brill USA, Boston, Mass.
- Grassl, H. (1976), The dependence of the measured cool skin of the ocean on wind stress and total heat flux, *Boundary Layer Meteorol.*, *10*, 465–474.
- Hasse, L. (1971), The sea surface temperature deviation and the heat flow at the air-sea interface, *Boundary Layer Meteorol.*, *1*, 368–379.
- Howard, L. N. (1966), Convection at high rayleigh numbers, in *Proceedings of the 11th International Congress of Applied Mechanics*, edited by H. Görtler, pp. 1109–1115, Springer, New York.
- Kent, E. C., T. N. Forrester, and P. K. Taylor (1996), A comparison of oceanic skin effect parameterizations using shipborne radiometer data, *J. Geophys. Res.*, *101*, 16,649–16,666.
- McLeish, W., and G. E. Putland (1975), Measurements of wind-driven flow profiles in the top millimeter of water, *J. Phys. Oceanogr.*, *5*, 516–518.
- Ocampo-Torres, F. J., M. A. Donelan, N. Merzi, and F. Jia (1994), Laboratory measurements of mass transfer of carbon dioxide and water vapour for smooth and rough flow conditions, *Tellus, Ser. B*, *46*, 16–32.
- Paulson, C. A., and T. W. Parker (1972), Cooling of a water surface by evaporation, radiation, and heat transfer, *J. Geophys. Res.*, *77*, 491–495.
- Paulson, C. A., and J. J. Simpson (1981), The temperature difference across the cool skin of the ocean, *J. Geophys. Res.*, *86*, 11,044–11,054.
- Robinson, I. S., N. Wells, and H. Charnock (1984), The sea surface thermal boundary layer and its relevance to the measurement of sea surface temperature by airborne and spaceborne radiometers, *Int. J. Remote Sens.*, *5*(1), 19–45.
- Saunders, P. (1967), The temperature at the ocean-air interface, *J. Atmos. Sci.*, *24*, 269–273.
- Schlüssel, P., W. J. Emery, H. Grassl, and T. Mammen (1990), On the bulk skin temperature difference and its impact on satellite remote sensing of sea surface temperature, *J. Geophys. Res.*, *95*, 13,341–13,356.
- Simpson, J. J., and P. Clayton (1980), Small-scale sea surface temperature structure, *J. Phys. Oceanogr.*, *10*, 399–410.
- Soloviev, A. V., and P. Schlüssel (1994), Parameterization of the cool skin of the ocean and of the air-ocean gas transfer on the basis of modelling surface renewal, *J. Phys. Oceanogr.*, *24*, 1339–1346.
- Ward, B. (2006), Near-surface ocean temperature, *J. Geophys. Res.*, *111*, C02004, doi:10.1029/2004JC002689.
- Ward, B., R. Wanninkhof, P. J. Minnett, and M. Head (2004), SkinDeEP: A profiling instrument for upper decimeter sea surface measurements, *J. Atmos. Oceanic Technol.*, *21*, 207–222.
- Wu, J. (1985), On the cool skin of the ocean, *Boundary Layer Meteorol.*, *31*, 203–207.

M. A. Donelan, Division of Applied Marine Physics, Rosenstiel School of Marine and Atmospheric Science, University of Miami, 4600 Rickenbacker Causeway, Miami, FL 33149–1098, USA.

B. Ward, Department of Ocean, Earth and Atmospheric Sciences, Old Dominion University, 4600 Elkhorn Avenue, Norfolk, VA 23539, USA. (bward@whoi.edu)